Catalysis Today 137 (2008) 162–166

Contents lists available at ScienceDirect

Catalysis Today

journal homepage: www.elsevier.com/locate/cattod

# Ir–C xerogels synthesized by sol–gel method for NO reduction

Zhi Liu [a,b], Aiqin Wang [a], Xiaodong Wang [a], Tao Zhang [a,*]

[a] State Key Laboratory of Catalysis, Dalian Institute of Chemical Physics, Chinese Academy of Sciences, Dalian 116023, China
[b] Graduate School of Chinese Academy of Sciences, Beijing 100039, China

ARTICLE INFO

*Article history:*
Available online 21 April 2008

*Keywords:*
Carbon xerogels
Iridium
NO reduction
Carbon monoxide
Sol–gel

ABSTRACT

Iridium–carbon (Ir–C) xerogels were synthesized via a one-pot sol–gel polycondensation of hexachloroiridic acid, resorcinol and formaldehyde, followed by carbonization in a nitrogen atmosphere at 500–1000 °C. The samples were characterized by various techniques including $N_2$ adsorption, XRD and TEM. The $N_2$ adsorption showed that the Ir–C samples were of microporous structures, and their specific surface areas increased with the pyrolysis temperature. Both the XRD and TEM revealed that the Ir particles in the Ir–C samples were highly dispersed in the carbon matrix, in contrast with the large Ir particles in the Ir/C sample which was obtained by impregnation. The Ir–C xerogels exhibited high activities and selectivities towards $N_2$ in the reduction of NO with carbon or CO. In particular, the Ir–C samples behaved much stably than the Ir/C, demonstrating the superiority of the one-pot synthesis method.

## 1. Introduction

Carbon gels are a kind of novel nanostructured carbon materials. They can be obtained by pyrolysis of organic gels, which are formed by the sol–gel polycondensation of certain organic monomers, such as resorcinol with formaldehyde, following Pekala's method [1,2]. The advantages of the carbon gels over the conventional carbon materials are the well-developed and controllable porosities, high surface areas, various shapes in macroscopic scale, and the easy incorporation of metal or metal oxide into the carbon framework. These unique properties make them promising materials as catalysts, catalyst supports and adsorbents as well. Over the past decade, a great deal of research effort has been made to understand how the synthesis parameters, such as the initial pH of the R-F solution, the catalyst employed, and the drying procedure, are affecting the resulting nanostructures, in particular the porosities and surface areas [3–8]. By contrast, the applications of carbon gels, especially in catalysis, are less exploited, and only a few examples have been reported so far [9–14].

Moreno-Castilla and co-workers firstly introduced transition metals into the organic aerogels and investigated the catalytic performances of Pt–carbon for xylene combustion [14]. Fortunately, they found that the activity of the catalysts increased with Pt particle size, thus the catalytic performance is stable, even in an oxidizing atmosphere. They also found that the transition metals incorporated into the carbon aerogels could catalyze the graphitization of carbon aerogels, which made it possible to produce graphite materials at 1000 °C [11]. The same group also investigated the catalytic performance of metal oxide–carbon aerogels for the isomerization of 1-butene [9].

In our previous work [15], we synthesized Cu–carbon and Co–carbon xerogels and investigated their potentials as catalysts for NO reduction. Although a very high NO conversion could be obtained at above 500 °C over these two metal-containing carbon xerogels, the activity decay still occurred with prolonging the time on stream due to the carbon gasification. To minimize the gasification of the synthesized carbon xerogels, either decreasing the reaction temperature or employment of an external reductant will be desirable. Based on our own previous work [16,17] and other literature reported work [18,19], highly dispersed iridium has been proved to be a very active and selective catalyst for NO reduction with hydrocarbons or CO even under the presence of oxygen in the feed stream. Therefore, in the present work, we incorporated Ir into the carbon xerogels and investigated its catalytic performances for NO reduction, with carbon itself or by addition of CO as the reductant.

## 2. Experimental

Ir-containing carbon xerogels (denoted as Ir–C) were prepared following the method described by Moreno-Castilla et al. [9]. Briefly, 6.160 g (0.056 mol) of resorcinol, 7.056 g (0.392 mol) of water and 0.537 g of hexachloroiridic acid ($H_2IrCl_6$, 44 wt.%) were mixed and stirred for 10 min. The amount of hexachlor-

---

* Corresponding author. Tel.: +86 411 84379015; fax: +86 411 84691570.
*E-mail address:* taozhang@dicp.ac.cn (T. Zhang).

0920-5861/$ – see front matter © 2008 Elsevier B.V. All rights reserved.
doi:10.1016/j.cattod.2008.03.004

oiridic acid added to the solution was calculated to obtain 1% by weight of the Ir in the initial solution. Then, 9.080 g (0.112 mol) of formaldehyde (37 wt.%) was added and the resulting solution was stirred until the organic gel formation. Afterwards, the organic gel was cured at 85 °C under vacuum for 7 days. The aqua-gels thus obtained were dried in $N_2$ atmosphere in a tubular furnace at 110 °C overnight to obtain the Ir-containing organic xerogels. Ir–C xerogels were finally obtained by pyrolyzing the Ir-containing organic xerogels at a specified temperature (500, 750 or 1000 °C) with a heating rate of 2 °C/min under $N_2$ for 5 h. A blank sample (C) was also prepared under the same conditions as those for the Ir–C, but without the addition of the Ir precursor. The exact iridium content of the Ir–C xerogel was determined by burning a fraction of it at 650 °C under air flow up to constant weight. The Ir–C or C xerogels will be referred to in the text by adding the carbonization temperature to the xerogel name, e.g., Ir–C1000 means a carbonization temperature of 1000 °C. For comparison, the catalyst Ir/C was also prepared by impregnating the above-prepared blank carbon xerogel (C1000) with the hexachloroiridic acid, and then by drying and calcination in $N_2$ at 500 °C for 3 h.

Textural characterizations were carried out by adsorption of $N_2$ at −196 °C on a Micromeritics ASAP 2010 apparatus. Before measurement, the samples were degassed firstly at 383 K for 3 h and then at 623 K for 5 h under vacuum. The specific surface areas ($S_{BET}$) of samples were calculated by BET equation, and the micropore surface area ($S_{mic}$) and micropore volume ($V_{mic}$) were determined by *t*-plot calculations.

Powder X-ray diffraction (XRD) patterns were collected with D/Max-βb diffractometer using Cu Kα radiation source ($\lambda$ = 0.15432 nm). A continuous mode was used to collect data from 10° to 80° of $2\theta$ at a scanning speed of 5°/min.

Transmission electron microscopy (TEM) images were obtained on a JEOL 2000EX electron microscope operating at an accelerating voltage of 120 kV. The samples were pulverized in an agate mortar, ultrasonic dispersed in ethanol and then dropped onto the carbon-coated copper grids prior to measurement.

The catalytic activities of the Ir–C xerogels for NO reduction were measured in a plug flow reactor using 0.2 g of the Ir–C sample in a gas mixture containing 2000 ppm NO (and 2000 ppm CO) in He at a total gas flow rate of 60 ml/min (corresponding to GHSV of 18,000 $h^{-1}$). The outlet gas mixture was analyzed by an on-line gas chromatograph (Agilent 6890N) equipped with a thermal conductivity detector (TCD), a Porapak QS column and a 13X molecular sieve column. NO conversion to $N_2$ ($Y_{N_2}$) or $N_2O$ ($Y_{N_2O}$), and the selectivity to $N_2$ ($S_{N_2}$) or $N_2O$ ($S_{N_2O}$) were defined as

$$Y_{N_2} = \frac{2N_2}{NO_{inlet}} \quad Y_{N_2O} = \frac{2N_2O}{NO_{inlet}}, \qquad S_{N_2}\,(\%) = \frac{Y_{N_2}}{Y_{N_2}+Y_{N_2O}} \times 100 \quad S_{N_2O}\,(\%) = \frac{Y_{N_2O}}{Y_{N_2}+Y_{N_2O}} \times 100$$

## 3. Results and discussion

### 3.1. Textural properties of Ir–C catalysts

Fig. 1 shows the $N_2$ adsorption–desorption isotherms of the C1000 and the three Ir–C samples which were obtained by pyrolysis at different temperatures. It can be seen that all of the four samples show typical type I isotherms, indicating their microporous structures. Table 1 lists some textural parameters of the four samples. A comparison between the C1000 and the Ir–C1000 in their textural properties shows that the incorporation of Ir only slightly decreased the BET surface area and the micropore volume. On the other hand, among the three Ir–C samples, we can clearly see that both the specific surface areas and the pore volumes increased with the pyrolysis temperature.

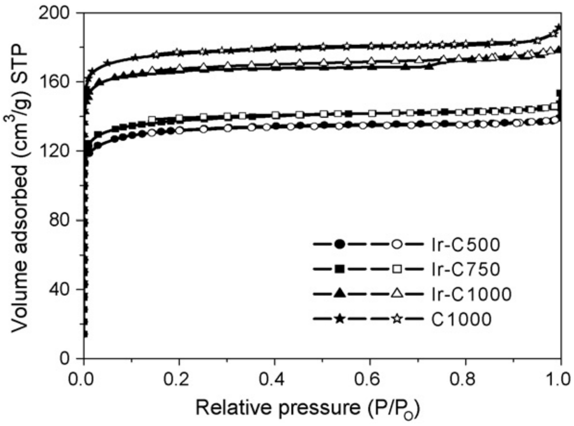

**Fig. 1.** Adsorption isotherms of $N_2$ on Ir–C samples prepared by pyrolysis at different temperatures. Closed symbols: adsorption isotherm; open symbols: desorption isotherm.

**Table 1**
Textural properties of Ir–C xerogels derived from sol–gel process

| Samples | Ir content[a] (%) | $S_{BET}$ ($m^2/g$) | $S_{mic}$ ($m^2/g$) | $V_{mic}$ ($cm^3/g$) |
|---|---|---|---|---|
| C1000 | 0 | 543 | 507 | 0.25 |
| Ir–C500 | 3.86 | 442 | 378 | 0.18 |
| Ir–C750 | 4.73 | 474 | 427 | 0.20 |
| Ir–C1000 | 4.91 | 488 | 439 | 0.21 |

[a] Metal content was determined by pyrolysis under air.

### 3.2. Characterization by XRD and TEM

Fig. 2 shows the XRD patterns of the three Ir–C samples. For comparison, those of the blank sample C1000 and the corresponding supported Ir/C1000 sample are also presented. All of the carbon xerogel samples, with or without Ir in the matrix, exhibit two broad peaks at ~22° and ~43° corresponding to amorphous carbon structure [11,15]. Besides, when Ir was introduced into the carbon matrix by impregnation (Ir/C1000), three strong diffraction peaks at $2\theta$ = 41°, 47° and 69° are observed, which are due to the presence of metallic Ir phase [19]. The sharp peaks of metallic Ir suggest that a poor dispersion of Ir particles on the Ir/C1000 sample, which is very different from other commercial metal

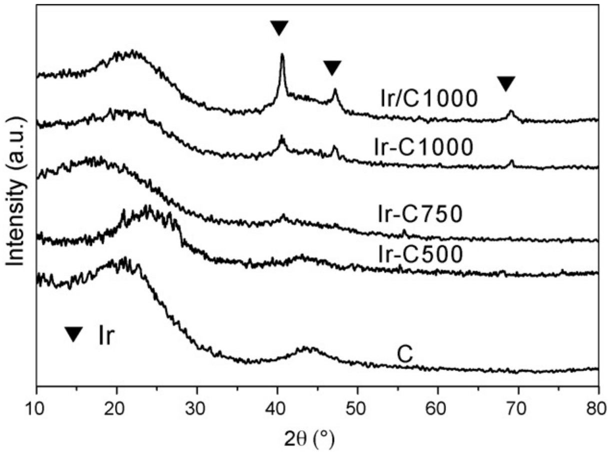

**Fig. 2.** X-ray diffraction patterns of different C and Ir–C samples.

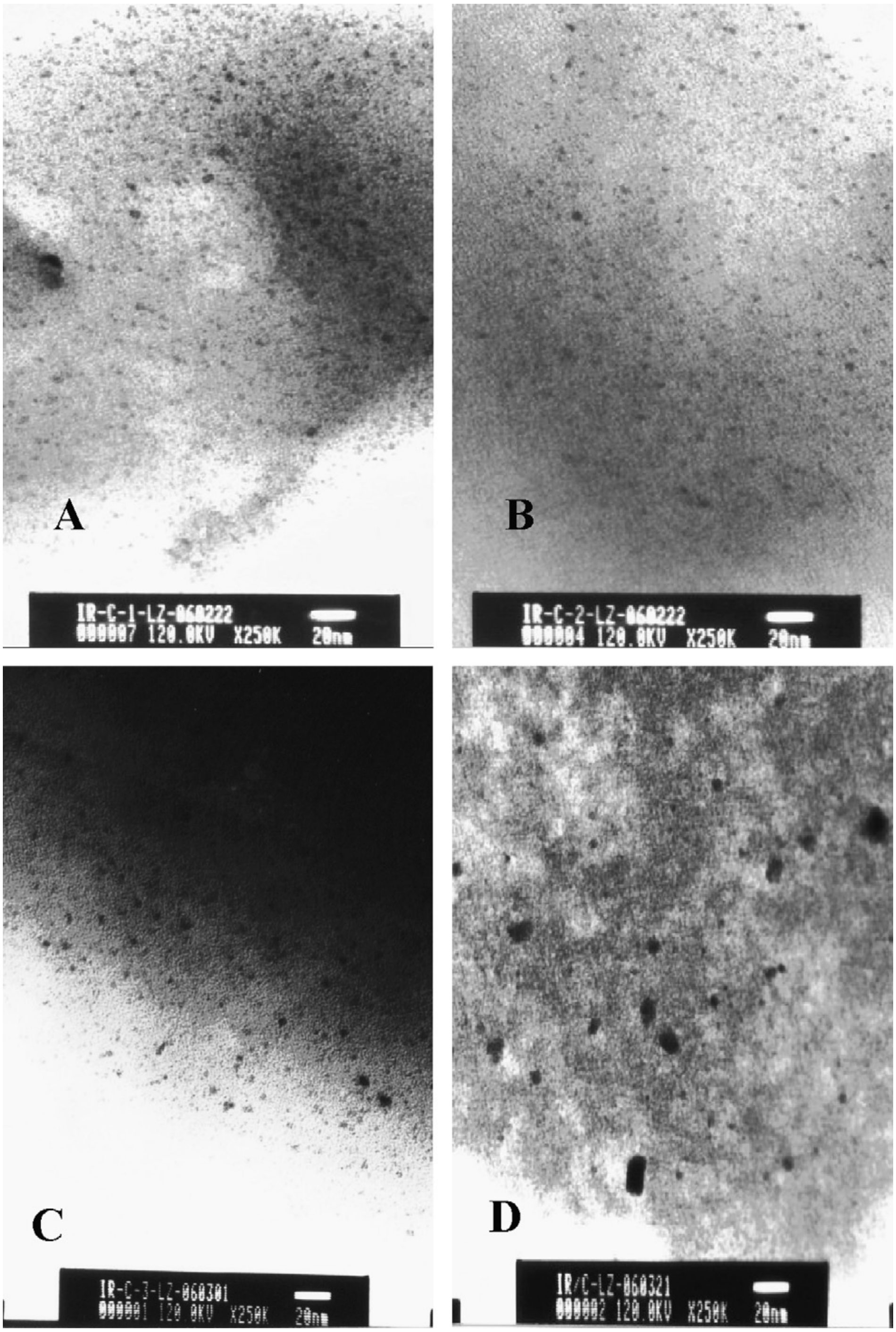

**Fig. 3.** TEM images of (A) Ir–C500; (B) Ir–C750; (C) Ir–C1000; and (D) Ir/C1000.

oxide supported catalysts, such as Ir/$Al_2O_3$ [20,21]. A possible reason for the poor dispersion of Ir on the Ir/C1000 is that the interaction between Ir and carbon is rather weak, which results in a serious aggregation of Ir particles upon heat treatment. On the other hand, when Ir was incorporated into the carbon matrix by our present one-pot sol–gel process, the XRD peaks corresponding to the metallic Ir had a drastic decrease in their intensities, as shown in Fig. 2. Furthermore, with decreasing pyrolysis temperature, the peak strength due to metallic Ir decreased, suggesting a higher dispersion degree of Ir can be obtained at a lower pyrolysis temperature.

To visually observe the size distributions of Ir particles on the three Ir–C samples, the samples were examined by TEM, as shown in Fig. 3. Ir particles with a size of 2–3 nm were uniformly distributed into the carbon matrix, which can be clearly seen on the Ir–C500 and Ir–C750 samples. When the carbonization temperature increased to 1000 °C (Ir–C1000), as shown in Fig. 3C, the size of iridium particles was slightly enlarged to 3–6 nm. However, for the sample Ir/C1000 (Fig. 3D), the Ir particle size was not uniform, ranging from a few nanometers to tens of nanometers. Evidently, both the TEM and XRD results manifested that the Ir–C xerogels prepared by one-pot sol–gel method have a

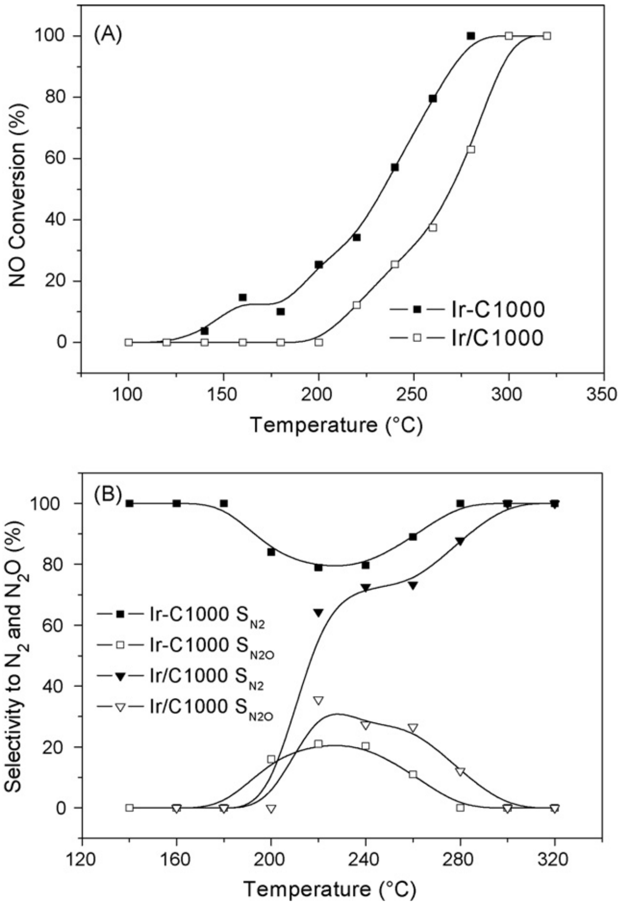

**Fig. 4.** (A and B) NO conversions and selectivities to $N_2$ and $N_2O$ with the reaction temperature over Ir–C1000 and Ir/C1000 catalysts. Gas composition: 2000 ppm NO in He.

high dispersion of Ir particles, even subjected to high-temperature pyrolysis. Such a feature, we believe, will be favorable for catalysis applications.

### 3.3. Catalytic performances of Ir–C xerogels

In our previous work [15], we have shown that Cu–C and Co–C xerogels exhibited high NO conversions at above 500 °C. However, the activity decay still occurred with prolonging the time on stream at such high temperatures due to the carbon gasification. In the present work, we used Ir–C as a catalyst for NO reduction, with an attempt to decrease the reaction temperature and to minimize the carbon gasification. Firstly, we investigated the NO reduction without the addition of external reductant. As shown in Fig. 4A, the Ir–C1000 presented a higher activity than the Ir/C1000; the NO conversion attained 100% at 275 °C over the former catalyst, which has a decrease of more than 200 °C compared with Cu–C and Co–C catalysts [15]. On the other hand, from the selectivities to $N_2$ and $N_2O$ (Fig. 4B), we can see that the selectivity to $N_2$ over the Ir–C1000 sample was higher than that over the Ir/C1000, at reaction temperatures below 300 °C. The selectivities to $N_2O$ attained their maxima (~20%) at around 220 °C over the two catalysts.

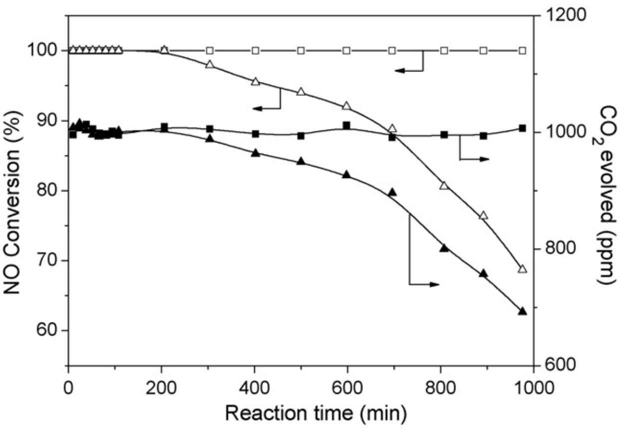

**Fig. 5.** NO conversion and evolved $CO_2$ versus reaction time at 320 °C on the Ir–C1000 (square) and Ir/C1000 (triangle) samples. Gas composition: 2000 ppm NO in He.

Fig. 5 compares the reaction stabilities of the two catalysts at the temperature of 320 °C. Similar to the Cu–C and Co–C [15], the Ir–C1000 showed a stable reactivity, with the NO conversion keeping at 100% over 1000 min run. In contrast, the Ir/C1000 presented a rapid decay in its reactivity and the NO conversion dropped from 100 to 68% after 1000 min of time on stream. This result again demonstrates that the one-pot synthesized metal–carbon catalysts possess high reactivities and stabilities, which should be attributed to the high dispersion of metal particles in the carbon matrix and the intimate contact between carbon and the metal active sites. Meanwhile, the amount of $CO_2$ evolved is found to be almost a half of the amount of NO converted, implying the following reaction mainly occurred between the carbon xerogel and NO:

$$2NO + C \rightarrow N_2 + CO_2$$

Evidently, under our present conditions, the carbon xerogel was consumed just for the NO conversion, and excess gasification of carbon did not occur.

Subsequently, we investigated the NO reduction with CO over the Ir–C catalysts. For this reaction, there are two possible routes:

$$\text{Route1} : 2NO + CO \rightarrow N_2O + CO_2$$

$$\text{Route2} : 2NO + 2CO \rightarrow N_2 + 2CO_2$$

Fig. 6 shows the temperature-dependence profiles of NO conversions to $N_2$ or $N_2O$ over the four Ir-containing carbon xerogels. It can be seen that in the whole temperature range investigated, NO was converted predominantly to $N_2$ and only a minor part was converted to $N_2O$. Meanwhile, we can see that all the three Ir–C catalysts exhibited higher activities and selectivities to $N_2$ than the Ir/C1000. For example, the NO conversion to $N_2$ at 160 °C over the Ir–C1000 sample was 54%, while it was only 8.7% at the same temperature over the Ir/C1000 sample. On the other hand, the production of $N_2O$ over the Ir–C1000 was significantly lower than that over the Ir/C1000. Moreover, comparing Figs. 6 and 4A, it can be seen that with the presence of external reductant CO, the temperature for complete NO conversion to $N_2$ was further decreased to 225 °C. This temperature is even lower than that for NO + CO reaction over Rh catalysts [22], indicating that our Ir–C catalysts are very active and selective for NO reduction by CO.

Although the Ir–C xerogels have shown good performances for the NO + CO reaction, it should be pointed out that under the presence of $O_2$ in the reaction stream, the deactivation induced by the continuous burning-off of the carbon matrix is inevitable. To avoid the decay of Ir–C xerogels caused by the carbon combustion and apply it effectively, we suggested that employing this material in a reaction with reductive atmosphere is more suitable than in an oxidizing one.

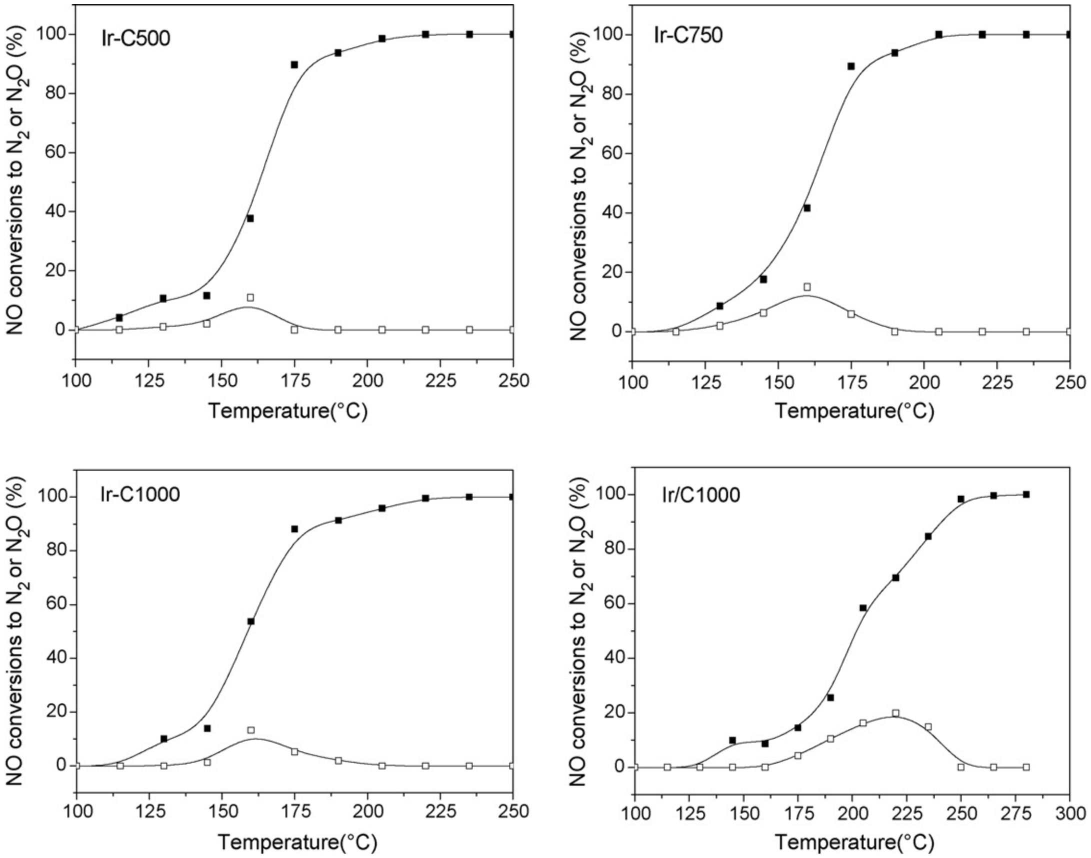

**Fig. 6.** NO conversion to $N_2$ (closed symbols) and $N_2O$ (open symbols) as a function of reaction temperatures over three Ir–C catalysts and Ir/C1000 catalyst. Reaction conditions: 2000 ppm NO, 2000 ppm CO and He as balance.

## 4. Conclusion

A new type of microporous iridium–carbon xerogels have been synthesized from the one-pot reaction of hexachloroiridic acid, resorcinol and formaldehyde. For this composite material, metallic Ir nanoparticles were highly dispersed in the carbon matrix, and exhibited high activity and selectivity for NO reduction with CO. In particular, the Ir–C xerogels showed superior stabilities to the Ir/C xerogels in the reaction. Even though, the deactivation induced by the continuous burning-off of the carbon matrix in the presence of oxygen is inevitable. Therefore, such Ir–C xerogels will be more suitable for those reactions in a reductive atmosphere.

## Acknowledgement

Financial support from the National Science Foundation of China for Distinguished Young Scholars (20325620) is gratefully acknowledged.

## References

[1] R.W. Pekala, J. Mater. Sci. 24 (1989) 3221.
[2] R.W. Pekala, C.T. Alviso, F.M. Kong, S.S. Hulsey, J. Non-Cryst. Solids 145 (1992) 90.
[3] H. Tamon, H. Ishizaka, M. Mikami, M. Okazaki, Carbon 35 (1997) 791.
[4] H. Tamon, H. Ishizaka, T. Yamamoto, T. Suzuki, Carbon 37 (1999) 2049.
[5] T. Yamamoto, T. Sugimoto, T. Suzuki, S.R. Mukai, H. Tamon, Carbon 40 (2002) 1345.
[6] R. Kocklenberg, B. Mathieu, S. Blacher, R. Pirard, J.P. Pirard, R. Sobry, G. Van den Bossche, J. Non-Cryst. Solids 225 (1998) 8.
[7] T. Yamamoto, T. Nishimura, T. Suzuki, H. Tamon, J. Non-Cryst. Solids 288 (2001) 46.
[8] S.A. Al-Muhtaseb, J.A. Ritter, Adv. Mater. 15 (2003) 101.
[9] C. Moreno-Castilla, F.J. Maldonado-Hodar, J. Rivera-Utrilla, E. Rodroguez-Castellon, Appl. Catal. A 183 (1999) 345.
[10] F.J. Maldonado-Hodar, C. Moreno-Castilla, J. Rivera-Utrilla, M.A. Ferro-Garcıa, Stud. Surf. Sci. Catal. B 30 (2000) 1007.
[11] F.J. Maldonado-Hodar, C. Moreno-Castilla, J. Rivera-Utrilla, Y. Hanzawa, Y. Yamada, Langmuir 16 (2000) 4367.
[12] M.L. Rojas-Cervantes, L. Alonso, J. Diaz-Teran, A.J. Lopez-Peinado, R.M. Marín-Aranda, V. Gomez-Serrano, Carbon 42 (2004) 1582.
[13] F.J. Maldonado-Hodar, C. Moreno-Castilla, A.F. Perez-Cadenas, Appl. Catal. B 54 (2004) 217.
[14] A.F. Perez-Cadenas, F. Kapteijn, J.A. Moulijn, F.J. Maldonado-Hodar, F. Carrasco-Marin, C. Moreno-Castilla, Carbon 44 (2006) 2359.
[15] Z. Liu, A.Q. Wang, X.D. Wang, T. Zhang, Carbon 44 (2006) 2345.
[16] A.Q. Wang, D.B. Liang, T. Zhang, Appl. Catal. B 32 (2001) 205.
[17] A.Q. Wang, L. Ma, Y. Cong, T. Zhang, D.B. Liang, Appl. Catal. B 40 (2003) 319.
[18] M. Ogura, A. Kawamura, M. Matsukata, E. Kikuchi, Chem. Lett. (2000) 146.
[19] T. Nakatsuji, Appl. Catal. B 25 (2000) 163.
[20] X.W. Chen, T. Zhang, M.Y. Zheng, L.G. Xia, T. Li, W.C. Wu, X.D. Wang, C. Li, Ind. Eng. Chem. Res. 43 (2004) 6040.
[21] X.W. Chen, T. Zhang, M.Y. Zheng, Z.L. Wu, W.C. Wu, C. Li, J. Catal. 224 (2004) 473.
[22] F. Fajardie, J.F. Tempere, J.M. Manoli, O. Touret, G. Blanchard, G.D. Mariadassou, J. Catal. 179 (1998) 469.